# Adsorption of lead(II) ions onto 8-hydroxy quinoline-immobilized bentonite

A. Safa Özcan, Özer Gök, Adnan Özcan *

*Department of Chemistry, Faculty of Science, Anadolu University, Yunusemre Campus, 26470 Eskişehir, Turkey*

## ARTICLE INFO

## ABSTRACT

In this study, the immobilization of 8-hydroxy quinoline onto bentonite was carried out and it was then used to investigate the adsorption behavior of lead(II) ions from aqueous solutions. The changes of the parameters of pH, contact time, initial lead(II) ions concentration and temperature were tested in the adsorption experiments. The XRD, FTIR, elemental and thermal analyses were done to observe the immobilization of 8-hydroxy quinoline onto natural bentonite. The adsorption was well described by the Langmuir adsorption isotherm model at all studied temperatures. The maximum adsorption capacity was $142.94 \, mg \, g^{-1}$ from the Langmuir isotherm model at $50\,^\circ C$. The thermodynamic parameters implied that the adsorption process is spontaneous and endothermic. The kinetic data indicate that the adsorption fits well with the pseudo-second-order kinetic model. 8-Hydroxy quinoline-immobilized bentonite can be used as well respective adsorbent for the removal of the heavy metal pollutants according to the results.

## 1. Introduction

Lead is harmful to humans, plants and animals. The lead poisoning can cause hypertension, nephritis, abdominal pain, constipation, cramps, nausea, vomiting, behavioral changes, learning disabilities, reading problems, development defects and language difficulties. Major lead pollution has been through in the manufacture of storage batteries, painting pigments, ammunition, solder, plumbing fixtures, automobiles, cable coverings, radioactivity shields, caulking and bearings [1,2].

Lead ions concentrations approach $200–500 \, mg \, dm^{-3}$ in the industrial wastewaters. This value is very high in relation to the water quality standards and it should be reduced to a range of $0.1–0.05 \, mg \, dm^{-3}$ [3,4].

Although the traditional treatment methods such as precipitation, oxidation, reduction, electrochemical treatment, reverse osmosis, solvent extraction, adsorption, ion-exchange and evaporation can be used for the metal bearing effluents, most of these methods are expensive and difficult to apply [5]. Among these methods, adsorption has proved to be one of the most feasible, simple, selective, cost-effective, ease of operation and high efficient process for the removal of heavy metals from polluted sources. The most popular adsorbent for the adsorption process is activated carbon. It has a high surface area, high adsorption capacity and high degree of surface reactivity, whereas it is very expensive and there is a need for regeneration after each adsorption experiment [6,7]. In order to decrease the cost of treatment process, the scientists have been attempted to investigate inexpensive, efficient and easily available adsorbents. In this manner, biological-based materials such as *Cephalosporium aphidicola* [2], *Pinus sylvestris* [8], *Saccharomyces cerevisiae* [9], *Sargassum natans* [10], *Aspergillus niger* [11], *R. arrhizus* [12], and *Bacillus* sp. [13]; natural clay materials such as kaolinite [14–17], illite [18], bentonite [19,20], montmorillonite [14,17,21], zeolite [22,23] and sepiolite [24,25] have been used to remove lead(II) ions from aqueous solutions by adsorption. The chemical and pore structures of clays usually determine their adsorption ability [26]. Bentonite, which is predominantly montmorillonite clay, is used a wide range of industrial applications such as clarification of edible and mineral oils, paints, cosmetics and pharmaceuticals [27]. Bentonite is a 2:1 type of clay mineral and its unit layer structure consists of alumina octahedral sheet placed between two silica tetrahedral sheets. The isomorphous substitution of $Al^{3+}$ for $Si^{4+}$ in the tetrahedral layer and $Mg^{2+}$ for $Al^{3+}$ in the octahedral layer results in a negative surface charge on the bentonite. The charge imbalance is offset by exchangeable cations ($Na^+$ and $Ca^{2+}$, etc.) at the bentonite surface [28].

Since the natural clay minerals have the relatively low adsorption capacity, they can be modified to improve their adsorption ability. In this study, a chelating agent (8-hydroxy quinoline), which has a selective reactivity for the target metal ion, was immobilized in bentonite. 8-Hydroxy quinoline-immobilized ben-

* Corresponding author. Tel.: +90 222 3350580/4815; fax: +90 222 3204910.
*E-mail addresses:* asozcan@anadolu.edu.tr (A.S. Özcan), ogok1@anadolu.edu.tr (Ö. Gök), aozcan@anadolu.edu.tr (A. Özcan).

tonite (HQ-bentonite) was then used as an adsorbent because the information about the adsorption kinetics, isotherms and thermodynamics of this adsorbent was not found in the literature.

## 1.1. Equilibrium parameters of adsorption

Equilibrium data, which are generally known as the adsorption isotherms, are the main requirements to understand the adsorption mechanism. The traditional adsorption isotherm models, Langmuir [29], Freundlich [30] and Dubinin–Radushkevich (D–R) [31], are used to describe the equilibrium between adsorbed lead(II) ions onto HQ-bentonite ($q_e$) and lead(II) ions in solution ($C_e$) at a constant temperature.

The Langmuir adsorption isotherm model assumes that adsorption takes place at specific homogeneous sites within the adsorbent. This model can be applied successfully in many monolayer adsorption processes. The linear equation of the Langmuir isotherm model is [29]:

$$\frac{C_e}{q_e} = \frac{1}{q_{max}K_L} + \frac{C_e}{q_{max}} \tag{1}$$

where $q_e$ is the equilibrium lead(II) ions concentration on the adsorbent (mg g$^{-1}$), $C_e$ is the equilibrium lead(II) ions concentration in solution (mg dm$^{-3}$), $q_{max}$ is the monolayer adsorption capacity of the adsorbent (mg g$^{-1}$) and $K_L$ is the Langmuir constant (dm$^3$ mg$^{-1}$) and related to the free energy of adsorption. A plot of $C_e/q_e$ versus $C_e$ for the adsorption gives a straight line of slope $1/q_{max}$ and intercepts $1/q_{max}K_L$.

The effect of isotherm shape has been studied [32] with a view to predict whether an adsorption system is favorable or unfavorable. The main feature of the Langmuir isotherm can be expressed by means of '$R_L$', a dimensionless constant referred to as separation factor or equilibrium parameter. $R_L$ is calculated using the following equation:

$$R_L = \frac{1}{1 + K_L C_0} \tag{2}$$

where $C_0$ is the lead(II) ions concentration (mg dm$^{-3}$). As the $R_L$ values lie between 0 and 1, the related adsorption process is favorable [32].

The Freundlich isotherm is an empirical equation can be used to describe heterogeneous systems. The linear equation of the Freundlich adsorption model is [30]:

$$\ln q_e = \ln K_F + \frac{1}{n} \ln C_e \tag{3}$$

where $K_F$ (dm$^3$ g$^{-1}$) and $n$ (dimensionless) are the Freundlich adsorption isotherm constants, being indicative of the extent of the adsorption and the degree of nonlinearity, respectively. The plot of $\ln C_e$ versus $\ln q_e$ for the adsorption was employed to generate the intercept value of $K_F$ and the slope value of $n$, respectively.

The Dubinin–Radushkevich (D–R) isotherm model is more general than the Langmuir isotherm model due to the fact that it does not assume a homogeneous surface or constant adsorption potential. It was applied to distinguish between the physical and chemical adsorption. The linear equation of (D–R) isotherm model [31] is

$$\ln q_e = \ln q_m - \beta \varepsilon^2 \tag{4}$$

where $\beta$ is a constant connected with the mean free energy of adsorption per mole of the adsorbate (mol$^2$ kJ$^{-2}$), $q_m$ is the theoretical saturation capacity (mol g$^{-1}$), and $\varepsilon$ is the Polanyi potential, which is equal to $RT\ln(1 + 1/C_e)$, where $R$ (J mol$^{-1}$ K$^{-1}$) is the gas constant, and $T$ (K) is the absolute temperature. Hence by plotting

$\ln q_e$ versus $\varepsilon^2$ it is possible to generate the value of $q_m$ from the intercept, and the value of $\beta$ from the slope.

## 1.2. Thermodynamic parameters of adsorption

Since $K_L$ is the Langmuir constant and its dependence with temperature that can be used to estimate the thermodynamic parameters, such as changes in the Gibbs free energy ($\Delta G^\circ$), enthalpy ($\Delta H^\circ$) and entropy ($\Delta S^\circ$) associated to the adsorption process and were determined by using following equations:

$$\Delta G^\circ = -RT \ln K_L \tag{5}$$

$$\ln K_L = \frac{-\Delta G^\circ}{RT} = \frac{-\Delta H^\circ}{RT} + \frac{\Delta S^\circ}{R} \tag{6}$$

The plot of $\ln K_L$ as a function of $1/T$ yields a straight line from which $\Delta H^\circ$ and $\Delta S^\circ$ were calculated from the slope and intercept, respectively.

## 1.3. Kinetic parameters of adsorption

Adsorption kinetics is one of the most valuable characteristics to be responsible for the efficiency of adsorption. Various kinetic models such as the Lagergren first-order, pseudo-second-order and Elovich, and the intraparticle diffusion have been applied for the experimental data to predict to the adsorption kinetics. Among them the Lagergren first-order rate equation is [33]:

$$\ln(q_1 - q_t) = \ln q_1 - k_1 t \tag{7}$$

where $q_1$ and $q_t$ are the amounts of lead(II) ions adsorbed on the adsorbent at equilibrium and at various times $t$ (mg g$^{-1}$) and $k_1$ is the rate constant of the Lagergren first-order model for the adsorption process (min$^{-1}$). Values of $k_1$ can be calculated from the slope of the plots of $\ln(q_1 - q_t)$ versus $t$.

The pseudo-second-order kinetic model equation [34] is expressed as

$$\frac{t}{q_t} = \frac{1}{k_2 q_2^2} + \left(\frac{1}{q_2}\right) t \tag{8}$$

where $q_2$ is the maximum adsorption capacity (mg g$^{-1}$) and $k_2$ is the rate constant of the pseudo-second-order model for the adsorption process (g mg$^{-1}$ min$^{-1}$). Values of $k_2$ and $q_2$ can be calculated from the plot of $t/q_t$ against $t$.

The Elovich equation is generally expressed as follows [35]:

$$\frac{dq_t}{dt} = \alpha \exp(-\beta q_t) \tag{9}$$

To simplify the Elovich equation, Chien and Clayton [36] assumed $\alpha\beta t \gg 1$ and by applying the boundary conditions $q_t = 0$ at $t = 0$ and $q_t = q_t$ at $t = t$ Eq. (9) occurs [37]:

$$q_t = \left(\frac{1}{\beta}\right) \ln(\alpha\beta) + \left(\frac{1}{\beta}\right) \ln t \tag{10}$$

where $\alpha$ is the initial adsorption rate (mg g$^{-1}$ min$^{-1}$) and $\beta$ is the desorption constant (g mg$^{-1}$) for Elovich equation. The plot of $q_t$ versus $\ln(t)$ gives the $1/\beta$ and $1/\beta \ln(a\beta)$ from the slope and from the intercept, respectively.

The intraparticle diffusion equation [38] can be written as follows:

$$q_t = k_p t^{1/2} + C \tag{11}$$

where $C$ is the intercept and $k_p$ is the intraparticle diffusion rate constant (mg g$^{-1}$ min$^{-1/2}$).

The Lagergren first-order, pseudo-second-order and Elovich models cannot identify the diffusion mechanism. For this reason,

the kinetic results were then subjected to analyze by the intraparticle diffusion model. According to this model, the plot of uptake, $q_t$, versus the square root of time ($t^{1/2}$) should be linear if the intraparticle diffusion is involved in the adsorption process and if these lines pass through the origin then intraparticle diffusion is the rate-controlling step. The initial curved portion of the plots seems to be due to boundary layer adsorption and the linear portion to intraparticle diffusion, with the plateau corresponding to equilibrium [39–42]. However, neither plot passed through the origin, this is indicative of some degree of boundary layer control and this further shows that the intraparticle diffusion is not the only rate-limiting step, but also other kinetic models may control the rate of adsorption, all of which may be taking place simultaneously. The slope of linear portion from the figure can be used to derive values for the rate parameter, $k_p$, for the intraparticle diffusion model.

The validity of used kinetic models in this study can be quantitatively checked by using a normalized standard deviation $\Delta q$ (%) calculated by the following equation [43]:

$$\Delta q \ (\%) = \sqrt{\frac{\sum [(q_{exp} - q_{cal})/q_{exp}]^2}{n-1}} \times 100 \qquad (12)$$

where $n$ is the number of data points.

## 2. Experimental

### 2.1. Preparation of 8-hydroxy quinoline-immobilized bentonite

The adsorbent, which is HQ-bentonite, in this study, was prepared by using natural bentonite and 8-hydroxy quinoline. Bentonite was provided from Çanakkale-Turkey. It was crushed, ground, sieved through a 63-μm size sieve and samples collected from under the sieve and dried in an oven at 110 °C for 2 h before use.

Natural bentonite (30 g) was suspended in 0.8 dm³ of deionized water and its pH was adjusted to 4.77 with acetic acid and HQ-bentonite prepared by adding 8-hydroxyl quinoline at equally the cation exchange capacity of bentonite. The mixture was stirred for 72 h for the immobilization of 8-hydroxyl quinoline onto bentonite. This treatment method was successed, the solid phase, which contains 8-hydroxyl quinoline-immobilized bentonite, was separated by filtration and then washed three times with deionized water. It was crushed, ground, sieved through a 63-μm size sieve and samples collected from under the sieve and dried in an oven at 70 °C for 24 h prior to use.

### 2.2. Lead(II) ions solutions

A stock solution of lead(II) ions was prepared by dissolving as known amount of Pb(NO₃)₂ in deionized water and the stock solution was then diluted to the various concentrations between 100 and 300 mg dm⁻³ and the pH of the solutions was adjusted to desired values with 0.1 M HCl or 0.1 M NaOH or acetate buffer. Fresh dilutions were used for each experiment. All the chemicals used were in analytical grade.

### 2.3. Characterization

Natural bentonite was characterized with respect to its cation exchange capacity (CEC) by the methylene blue method [44] and it was found as 980 mmol kg⁻¹. The BET surface areas of natural- and HQ-bentonite were determined from N₂ adsorption isotherm with a surface area analyzer (Quantachrome Instruments, Nova 2200e) and the results were 67.49 and 45.69 m² g⁻¹, respectively.

The chemical analysis of natural bentonite was conducted using an energy-dispersive X-ray spectrometer (EDX-LINK ISIS 300) attached to a scanning electron microscope (SEM-Cam Scan S4). The crystalline phases present in bentonite were determined via X-ray diffractometry (XRD-Rigaku Rint 2000) using Cu K$_\alpha$ radiation.

Fourier transform infrared spectra of natural-, HQ-bentonite and lead(II) ions-loaded HQ-bentonite prepared as KBr discs were recorded in a PerkinElmer Spectrum 100 Model Infrared Spectrophotometer to observe immobilization of 8-hydroxyl quinoline onto bentonite.

The elemental analysis (Vario EL III Elemental Analyzer, Hanau, Germany) of HQ-bentonite was carried out to determine C/N ratio in HQ-bentonite. Thermal analysis (Setaram) was performed to observe the immobilization of 8-hydroxyl quinoline onto bentonite. The analyses for natural bentonite, 8-hydroxyl quinoline and HQ-bentonite were carried out in the temperature range 25–1000, 25–550, and 25–1000 °C, respectively, at a heating rate of 10 °C min⁻¹.

Zeta potential measurements of natural bentonite, HQ-bentonite and HQ-bentonite in the presence of lead(II) ions was determined by using a ZEN 3600 Model Zetasizer Nano-ZS connected with MPT-2 multipurpose automatic titrator (Malvern Inst. Ltd., UK). The optical device contains a 5 mW He–Ne (638 nm) laser. The sample of 0.1 g of suspensions of natural bentonite, HQ-bentonite and HQ-bentonite (in 50 mL of lead(II) ions solution) were sonicated for 10 min. The suspension was then kept still for 5 min to let larger particles settle. About 10 mL of clear supernatant was placed into the vial, which was connected with automatic titrator. The desired pH of the solution was kept constant during conditioning by introducing appropriate amounts of HCl or NaOH.

### 2.4. Adsorption studies

Adsorption experiments were firstly conducted with adsorbent in an Erlenmeyer on a magnetic stirrer to determine the optimum pH where the maximum adsorption was accomplished for lead(II) ions. The solution pH ranging from 1.5 to 5.5 was carefully adjusted by adding a small amount of HCl or NaOH or acetate buffer solution and measured using a pH meter (Fisher Accumet AB15), while 50 mL of 100 mg dm⁻³ lead(II) ions solutions contained in 100 mL Erlenmeyer flasks closed with stoppers were stirred using a magnetic stirrer.

The optimum pH was then determined as 5.5 and used throughout all adsorption experiments. Lead(II) ions concentrations ranging from 100 to 300 mg dm⁻³ were prepared and used to obtain the adsorption isotherm data on the adsorption process. The adsorption of lead(II) ions onto HQ-bentonite was done at constant temperatures of 20, 30, 40 and 50 °C for the adsorption isotherms. Once the optimum pH had been attained, the experiments were carried out at this pH value with increasing the periods of time (5–150 min) and temperatures of 20, 30, 40 and 50 °C, until no more lead(II) ions were removed from the aqueous phase and the equilibrium had been achieved. When the adsorption procedure completed in such time (60 min), the solutions were filtered and the equilibrium concentrations were then analyzed for residual lead(II) ions concentrations by using an atomic absorption spectrophotometer (PerkinElmer AAnalyst 800) with an air–acetylene flame. Deuterium background correction was used and the spectral slit width was 1.3 nm. The working current and wavelength were 7.5 mA and 283.3 nm, respectively. The instrument calibration was periodically checked by using standard metal solutions for every 15 reading. The amount of lead(II) ions adsorbed onto HQ-bentonite was determined by the difference between the initial and the remaining concentrations of lead(II) ions solution. The

adsorption capacity was determined by using the following equation taking into the concentration differences of the solution at the beginning and equilibrium accounts:

$$q_e = (C_i - C_e)\frac{V}{m} \tag{13}$$

where $C_i$ and $C_e$ are the initial and the equilibrium lead(II) ions concentrations ($mg\,dm^{-3}$), $V$ the volume of the solution ($dm^3$) and $m$ is the amount of adsorbent used (g).

### 2.5. Desorption studies

The recovery and reusability of the adsorbent material is an important parameter related to the application potential of adsorption processes. In this study, 8-hydroxy quinoline-immobilized bentonite subjected to 0.1 M HCl solution in order to determine desorption properties of HQ-bentonite. The bound lead(II) ions were eluted in 50 ml (S/L = 1) of the eluent. Each adsorption and desorption cycle was allowed 60 min of contact time and consecutive adsorption–desorption cycles were repeated five times using the same adsorbent in solutions containing adsorbent–lead(II) ions or adsorbent–desorbing agent for achieving adsorption or desorption equilibrium. The eluted adsorbent was washed repeatedly with deionized water to remove any residual desorbing solution and placed into metal solution for the next adsorption cycle.

## 3. Results and discussion

### 3.1. Characterization

#### 3.1.1. Chemical composition of bentonite

The chemical composition of natural bentonite was determined by using EDX analysis and it was given as follows (%): $SiO_2$: 70.75, $Al_2O_3$: 16.18, $K_2O$: 2.12, CaO: 1.62, MgO: 1.25, $Fe_2O_3$: 0.70, $TiO_2$: 0.18, $Na_2O$: 0.11 and loss of ignition: 6.63. This result indicates the presence of silica and alumina as major constituents along with traces of sodium, potassium, iron, magnesium, calcium, and titanium oxides in the form of impurities. XRD results combined with EDX analysis show that most of the silicon is in the form of bentonite. XRD also indicated the presence of free quartz in bentonite. It is, thus, expected that the adsorbate species will be removed mainly by $SiO_2$ and $Al_2O_3$.

The XRD patterns of natural bentonite and HQ-bentonite were recorded (Fig. 1) and their basal spaces were observed at 14.87 and 15.08 Å, respectively. The expansion in the basal spacing of the natural bentonite due to the intercalation of 8-hydroxy quinoline was calculated as $\Delta d = d - 14.87$ Å, where $d$ is the basal spacing of the HQ-immobilized bentonite and 15.08 Å is the thickness of a clay layer [45]. $\Delta d$ is found to be 0.21 Å. This result suggests that 8-hydroxy quinoline intercalate into the interlayers of bentonite and also agrees well with the FTIR and thermal analysis results.

#### 3.1.2. FTIR analysis

The FTIR spectra of natural bentonite, HQ-bentonite and lead(II) ions-loaded HQ-bentonite (Fig. 2) were taken in the range of 400–4000 $cm^{-1}$ and compared with each other to obtain information on the immobilization of the 8-hydroxy quinoline into the silicate lattice of bentonite and the nature of possible HQ-bentonite with metal ions interactions.

The absorption peaks were observed between 3421 and 3625 $cm^{-1}$, which is due to H–O–H stretching vibration bands of water molecules weakly hydrogen bonded to the Si–O surface in the natural bentonite (Fig. 2(a)) and HQ-bentonite (Fig. 2(b)) and their bending vibrations at 916 and 845 $cm^{-1}$. The bands between 1639 and 1643 $cm^{-1}$ also correspond to the –OH deformation of water to
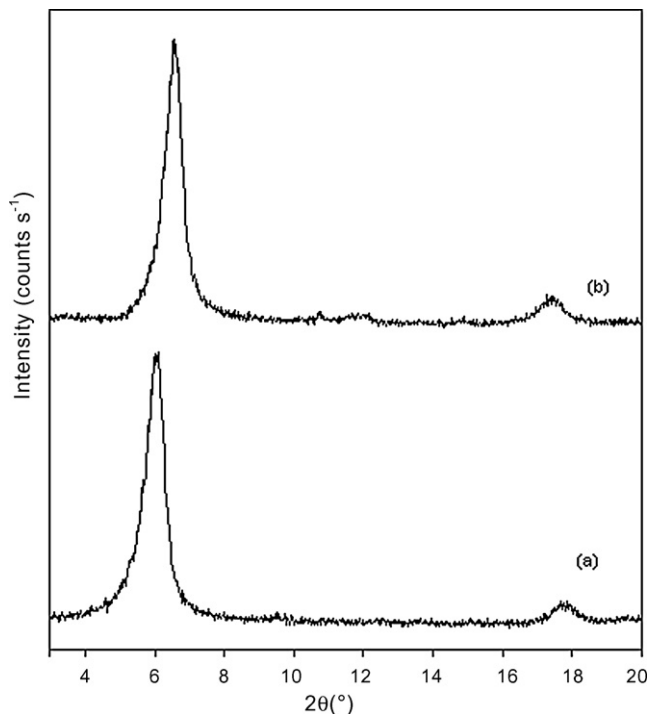


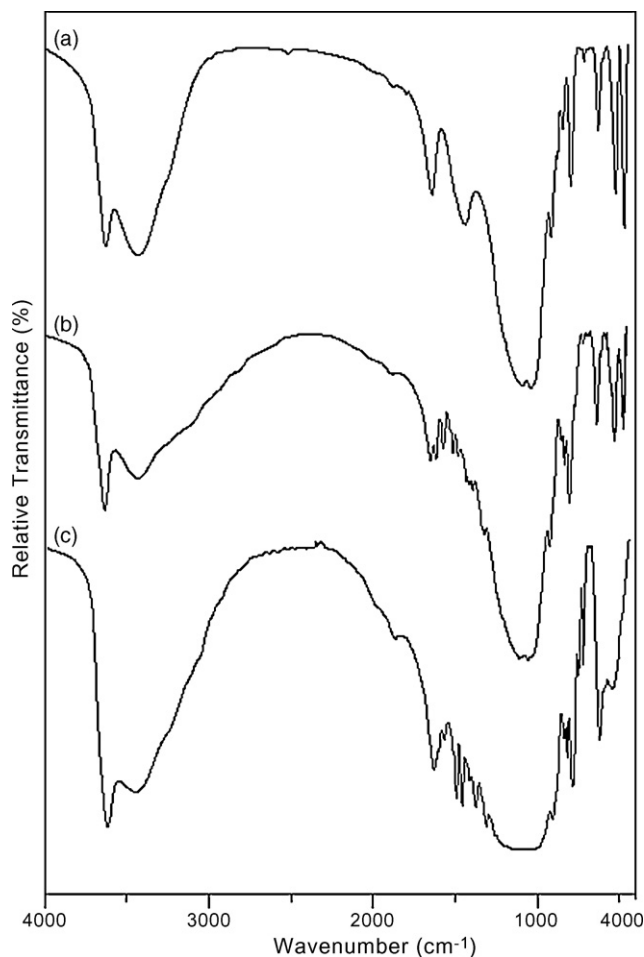Fig. 1. XRD patterns of (a) natural bentonite and (b) HQ-bentonite.



Fig. 2. FTIR spectra of (a) natural bentonite, (b) HQ-bentonite, (c) lead(II) ions-loaded HQ-bentonite.
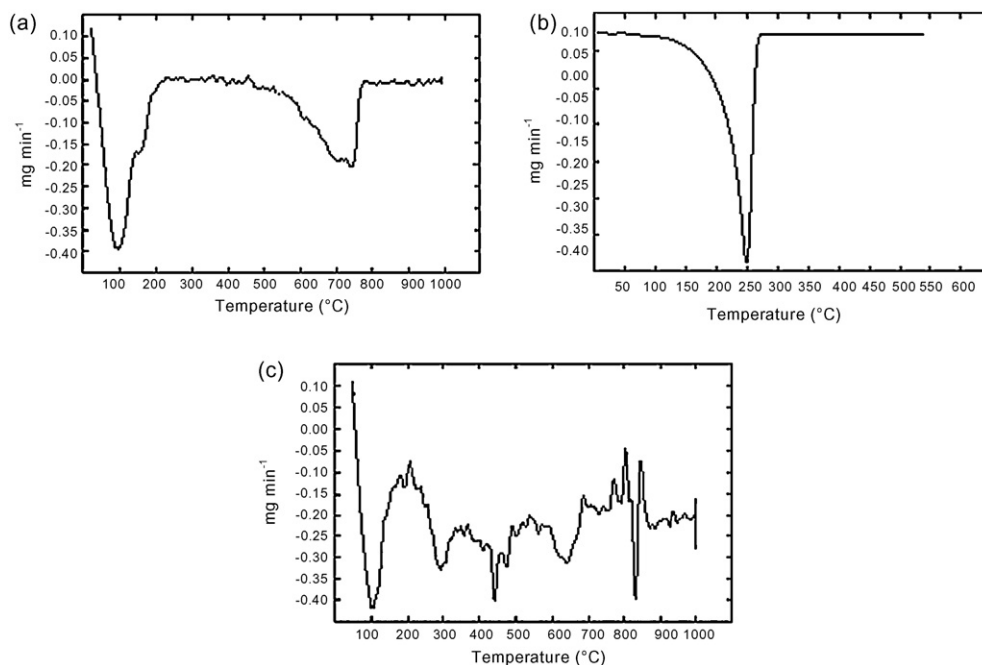
**Fig. 3.** Differential thermogravimetric (DTG) curves of: (a) natural bentonite, (b) 8-hydroxy quinoline and (c) HQ-bentonite.

observe natural bentonite and HQ-bentonite. The C–C and C–N ring stretching (skeletal) vibrations in the HQ-bentonite (Fig. 2(b)) were observed at 1563, 1503, 1383 and 1313 cm$^{-1}$ (four bands) and the ring bending vibration obtained at 823 cm$^{-1}$ [46], but these bands were not observed in the natural bentonite. This may be acceptable evidence for the immobilization of HQ onto natural bentonite. The intensities of above C–C and C–N ring stretching (skeletal) vibrations increased in the lead(II) ions-loaded HQ-bentonite (Fig. 2(c)). In addition the C–C and C–N ring stretching (skeletal) bands in the lead(II)-loaded HQ-bentonite (Fig. 2(c)) shifts 1574, 1499, 1385 and 1317 cm$^{-1}$ and the ring bending vibration moves at 825 cm$^{-1}$. The movement and the increment of the peak intensities in these bands indicate the interaction between the HQ-bentonite and the metal ions. Therefore, HQ-bentonite provides more adsorption sites for lead(II) ions.

The Si–O coordination bands at 1087 and 1039 cm$^{-1}$ are observed as a result of the Si–O vibrations. The deep band at around 1039 cm$^{-1}$ represents the stretching of Si–O in the Si–O–Si groups of the tetrahedral sheet. The bands at 523 and 467 cm$^{-1}$ are due to Si–O–Al (octahedral) and Si–O–Si bending vibrations, respectively, for natural- and HQ-bentonite. The Si–O stretching vibration at around 1039 cm$^{-1}$ shifts 1103 cm$^{-1}$ after lead(II) ions loaded. It confirms that there is an interaction between HQ-bentonite and lead(II) ions.

### 3.1.3. Elemental and thermal analysis

The ratio of C/N for HQ-bentonite from elemental analysis results is 7.702 and the calculated value of C/N ratio is 7.717. The percentage of 8-hydroxy quinoline immobilization onto bentonite is 11.46. This result confirms that the intercalation of 8-hydroxy quinoline molecules between bentonite layers occurs and this is also consistent with the above FTIR analysis results.

The thermal analysis curves of the natural bentonite, 8-hydroxy quinoline and HQ-bentonite were illustrated in Fig. 3(a–c), respectively. The DTG peak between 250 and 350 °C, centered at 300 °C, was observed in HQ-bentonite and it confirms the immobilization of 8-hydroxy quinoline onto bentonite, whereas this peak is not observed in the natural bentonite.

### 3.2. Zeta potential measurements

The zeta potential of natural bentonite, HQ-bentonite and HQ-bentonite (in lead(II) ions solution) was illustrated in Fig. 4, as a function of suspension pH. As shown in Fig. 4(a) and (b), natural bentonite and HQ-bentonite have no point of zero charge (pH$_{pzc}$) and exhibit negative zeta potential values at all studied pH values.
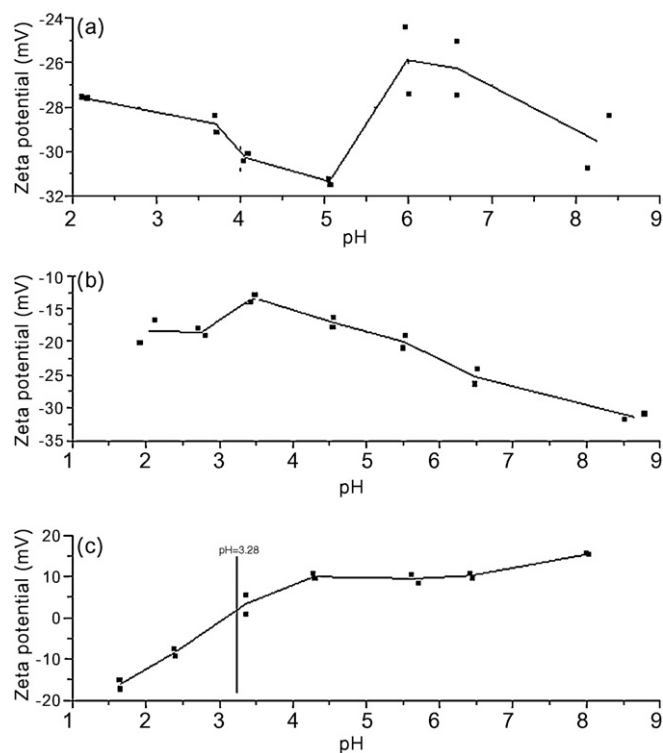


**Fig. 4.** The zeta potential of: (a) natural bentonite, (b) HQ-bentonite and (c) lead(II) ions-loaded HQ-bentonite solution as a function of pH.

This result agrees with those obtained from electrokinetic measurements of the other clay minerals in the literature [47–50]. The origin of this charge is still a controversial issue, whereas the majority of evidence suggests that this charge arises from isomorphic transactions, defects in the crystal lattice, broken particle edges, and structural hydroxyl groups. The electrical charge at the oxide surface/aqueous phase to protonation/deprotonation of the surface hydroxyl can be ascribed as [51]:

$$M–OH + H^+ \rightleftharpoons M–OH_2^+ \tag{14}$$

$$M–OH + OH^- \rightleftharpoons M–O^- + H_2O \tag{15}$$

where M is the central metal ion (Si or Al) and at $pH_{pzc}$:

$$[M–O^-] = [M–OH_2^+] \tag{16}$$

Since there was no $pH_{pzc}$, the reaction responsible for the surface charge of the solid is mainly the reaction in Eq. (15). When pHs of the natural bentonite and HQ-bentonite dispersions (Fig. 4(a) and (b)) were increased, the negative charge increases. Zeta potential–pH curves reflect a decrease on the negativity of charges. The zero point could not obtain for both of bentonite dispersion (absence of lead(II) ions) due to the neutrality of the clay particles could not be obtained. The repulsion between clay particles increases with increasing in pH [52].

The zeta potential is important in the case of HQ-bentonite in lead(II) ions solution and it is dependent on the pH (Fig. 4(c)). The point of zero charge, where the colloidal system is least stable [53], was measured as 3.28 for HQ-bentonite in lead(II) ions solution. After this point (pH > 3.28), the surface charge becomes increasingly positive, but the natural bentonite and HQ-bentonite (the absence of lead(II) ions) have a negative charge (Fig. 4(a) and (b)), while lead(II) ions tends to form a cationic species and consequently, has a positive surface charge (Fig. 4(c)), thus the electrostatic interactions between the surface and lead(II) ions complexes are considerable. Therefore, changes to the sign of the zeta potential of HQ-bentonite in the presence of lead(II) ions can be directly related to the specific adsorption of cationic lead(II) ions [51]. It was assumed that $PbOH^+$, $Pb(OH)_2$ and $Pb(OH)_3^-$ exist at low concentration of lead ($<1 \times 10^{-5}$ M) and at various pH. Higher lead concentrations ($>1 \times 10^{-5}$ M) promote the formation of complex species containing more than one lead ion, that include $Pb_2OH^{3+}$, $Pb_3(OH)_4^{2+}$, $Pb_4(OH)_4^{4+}$, $Pb_6(OH)_8^{4+}$ [54,55]. According to Qiu et al. [56] lead exists predominantly as cations. At pH ≤ 6.01, Pb exists at >89% of total lead(II) ions, indicating its predominance in acidic solution. The species of $Pb(OH)_2$, $Pb(OH)_3^-$, $Pb_2(OH)^{3+}$, $Pb_3(OH)_4^{2+}$, and $Pb_4(OH)_4^{4+}$ do not virtually exist in acidic solution. At pH 7.05, the percentage of lead(II) ions decreases to ~76%, while $PbOH^+$ rises to ~16%. At pH 8.85, lead(II) ions decreases sharply to ~4% and $PbOH^+$ increases to ~55%. According to the percentage and valence of individual species, the total positive charge of lead(II) species remains constant for the pH range of 2.85–6.01. When pH is raised to 7.05, there is a 7.8% reduction in total positive charge, apparently due to the decrease in divalent lead(II) and the formation of monovalent $PbOH^+$.

### 3.3. Effect of pH

The pH of aqueous solution has been known as the most important variable governing heavy metal adsorption onto adsorbent. This is partly because hydrogen ions themselves are strongly competing with adsorbates. Fig. 5 shows the effect of pH on the removal of lead(II) ions onto natural bentonite and HQ-bentonite from aqueous solutions. It can be easily seen from Fig. 5 that the adsorption capacities increased almost the same amount for both of the samples up to pH 4.0. After pH 4.0, uptakes increase sharply up to pH
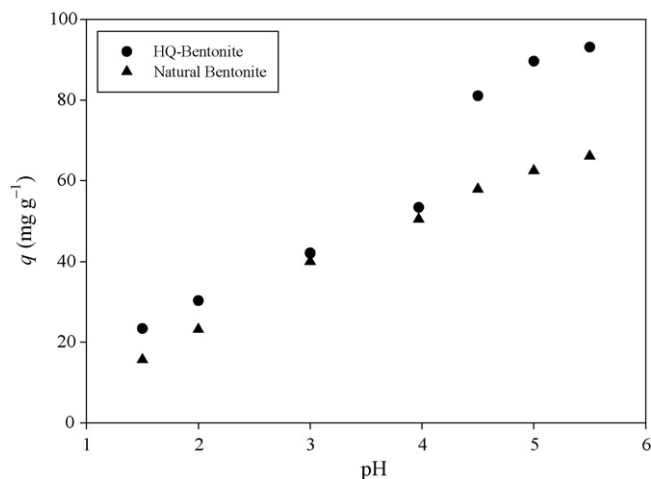


**Fig. 5.** Effect of pH for the adsorption of lead(II) ions onto natural bentonite and HQ-bentonite at 20 °C.

5.0 for HQ-bentonite and then it was stable up to pH 5.5 since more metal-binding sites could be exposed and carried negative charges, with subsequent attraction of metal ions with positive charge and adsorption onto the adsorbent surface. Experiments were not carried out with the pH values above 5.5 due to the fact that metal precipitation appeared at higher pH values and interfered with the accumulation or adsorbent deterioration [57].

### 3.4. Effect of contact time

The influence of contact time on the adsorption of lead(II) ions onto HQ-bentonite (Fig. 6) was investigated at various temperatures, i.e. 20, 30, 40 and 50 °C. It is easily seen from Fig. 6 that the amount of adsorption increased with increasing the contact time. The maximum adsorption capacity was observed after 60 min, beyond which there was almost no further an increase in the adsorption. This was therefore fixed as the equilibrium contact time.

### 3.5. Effect of temperature on metal removal

The equilibrium adsorption capacity of lead(II) ions onto HQ-bentonite was favored at higher temperatures as can be seen from
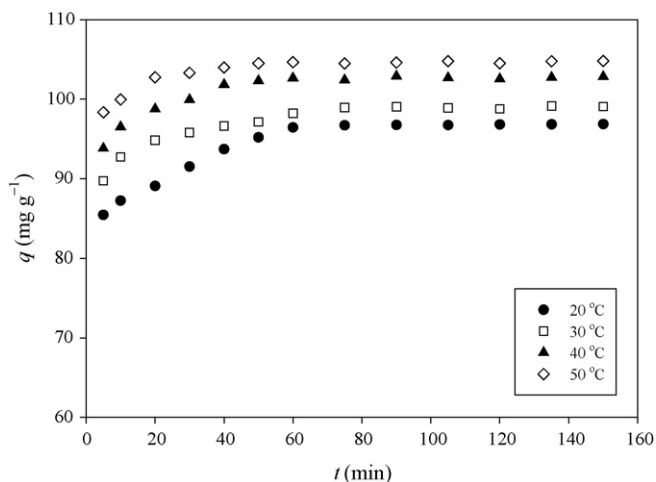


**Fig. 6.** Effect of contact time for the adsorption of lead(II) ions onto HQ-bentonite at various temperatures.

**Table 1**
Isotherm constants for the adsorption of lead(II) ions onto HQ-bentonite at various temperatures

| $t$ (°C) | Langmuir | | | | Freundlich | | | Dubinin–Radushkevich (D–R) | | |
|---|---|---|---|---|---|---|---|---|---|---|
| | $q_{max}$ (mg g$^{-1}$) | $K_L$ (dm$^3$ mg$^{-1}$) | $R_L$ | $r_L^2$ | $n$ | $K_F$ (dm$^3$ g$^{-1}$) | $r_F^2$ | $q_{max}$ (mg g$^{-1}$) | $\beta$ (mol$^2$ kJ$^{-2}$) | $r_{D-R}^2$ |
| 20 | 139.08 | 0.103 | $1.46 \times 10^{-2}$ | 0.998 | 6.154 | 58.73 | 0.977 | 218.82 | $1.63 \times 10^{-3}$ | 0.982 |
| 30 | 139.48 | 0.163 | $9.32 \times 10^{-3}$ | 0.998 | 7.862 | 71.84 | 0.988 | 198.00 | $1.16 \times 10^{-3}$ | 0.991 |
| 40 | 141.43 | 0.193 | $7.88 \times 10^{-3}$ | 0.998 | 8.830 | 78.13 | 0.992 | 190.61 | $9.42 \times 10^{-4}$ | 0.989 |
| 50 | 142.94 | 0.307 | $4.96 \times 10^{-3}$ | 0.998 | 11.96 | 91.91 | 0.984 | 173.95 | $6.14 \times 10^{-4}$ | 0.970 |

Fig. 6. This may indicate that adsorption of lead(II) ions onto HQ-bentonite is endothermic. An increase in the temperature from 20 to 50 °C leads to an increase in the amount of adsorption from 96.43 to 104.64 mg g$^{-1}$ at an equilibrium time of 60 min. Below equilibrium time, an increase in the temperature leads to an increase in lead(II) ions adsorption, which indicates temperature depending process. After the equilibrium attained, the uptake increases with increasing temperature, this effect may be explained by availability of more in active sites of adsorbent, the enlargement of pore size and/or activation of the adsorbent surface at higher temperatures. This could also be due to the increment in mobility of lead(II) ions from the bulk solution towards the adsorbent surface and enhanced the penetration within HQ-bentonite. [58].

### 3.6. Effect of initial lead(II) ions concentration

The results of the experiments with varying initial lead(II) ions concentrations (100–150 mg dm$^{-3}$) are illustrated in Fig. 7. When the initial lead(II) ions concentration was increased from 100 to 150 mg dm$^{-3}$, the amount of adsorbed lead(II) ions raised from 86.32 to 106.75 mg g$^{-1}$ at 20 °C. According to these results, the initial lead(II) ions concentration plays an important role in the adsorption capacities.

### 3.7. Adsorption isotherms

The equilibrium adsorption isotherms are known one of the most important data to understand the mechanism of the adsorption. Various isotherm equations are chosen in this study, which are namely the Langmuir, Freundlich and Dubinin–Radushkevich (D–R) isotherms. The plots of linear form of Langmuir, Freundlich and Dubinin–Radushkevich (D–R) adsorption isotherms of lead(II) ions obtained at various temperatures, which are 20, 30, 40 and 50 °C, are depicted in Figs. 8–10. All of the isotherm model parameters for
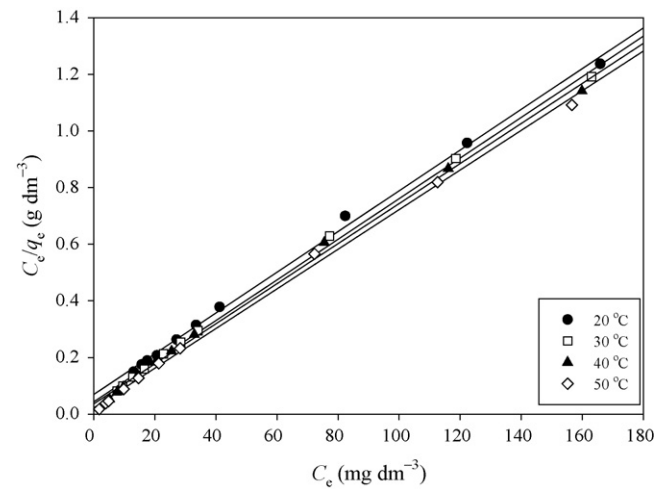
**Fig. 8.** Langmuir plots for the adsorption of lead(II) ions onto HQ-bentonite at various temperatures.

the adsorption of lead(II) ions onto HQ-bentonite are summarized in Table 1. It is evident from these data that the adsorption of lead(II) ions onto HQ-bentonite is fitted well to the Langmuir isotherm model than that of the Freundlich and D–R isotherm models, as indicated by the numerical values of the correlation coefficients ($r^2$) in Table 1.

The maximum adsorption capacity ($q_{max}$) of adsorbent calculated from Langmuir isotherm equation defines the total capacity of the adsorbent for lead(II) ions. The adsorption capacity of adsorbent increased with increasing the temperature. The highest value of $q_{max}$ obtained at 50 °C is 142.94 mg g$^{-1}$. It appears to be the highest in comparison with the uptake obtained at the other temperatures
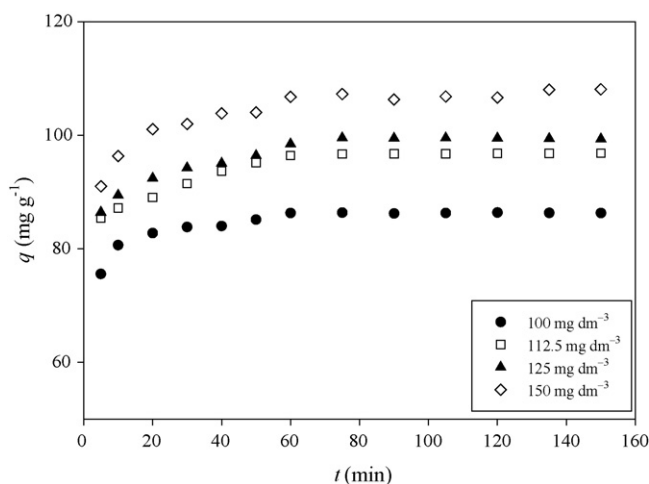
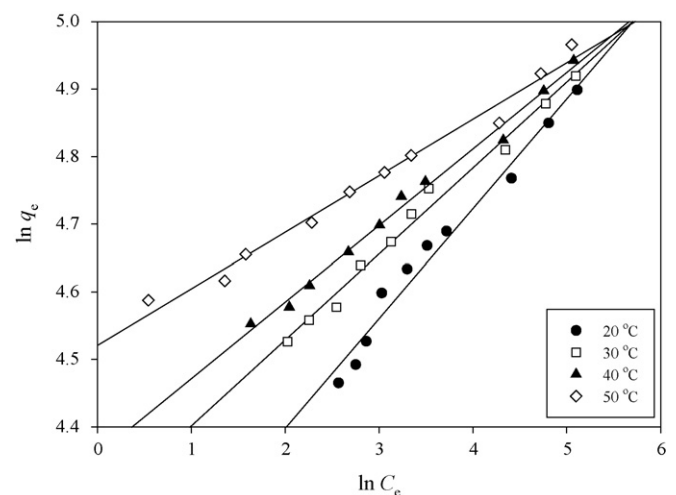**Fig. 7.** The effect of initial concentrations for the adsorption of lead(II) ions onto HQ-bentonite at 20 °C.

**Fig. 9.** Freundlich plots for the adsorption of lead(II) ions onto HQ-bentonite at various temperatures.
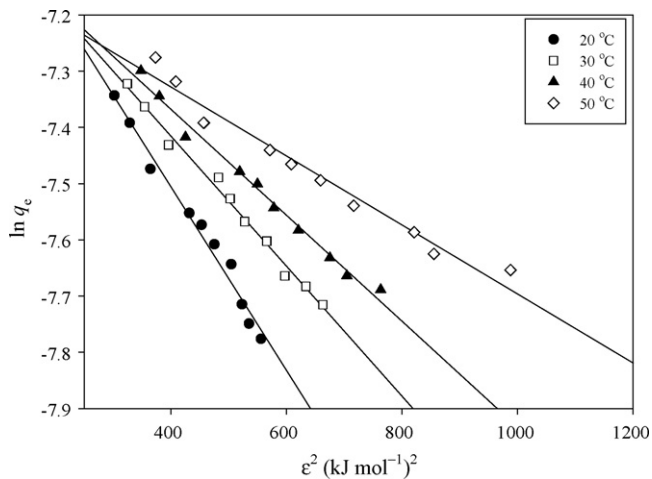
**Fig. 10.** Dubinin–Radushkevich (D–R) plots for the adsorption of lead(II) ions onto HQ-bentonite at various temperatures.

(Table 1). In addition to, the maximum adsorption capacity of HQ-bentonite obtained for lead(II) ions in this study was found to be comparable and the highest for all of corresponding clay-related adsorbents reported in the literature [16,17,19,23,59–64] (Table 2).

The value of $R_L$ calculated from Eq. (2) is incorporated in Table 1. As the $R_L$ values lie between 0 and 1, the adsorption process is favorable [32]. Further, the $R_L$ values for this study at all studied temperatures are between $9.32 \times 10^{-3}$ and $1.46 \times 10^{-2}$, therefore, the adsorption is favorable.

The Freundlich constant $K_F$ indicates the adsorption capacity of the adsorbent and the values of $K_F$ at equilibrium at all temperatures lie the range of 58.73–91.91 $dm^3 \, g^{-1}$. The other Freundlich constant $n$ is a measure of the deviation from linearity of the adsorption and the numerical values of $n$ at all temperatures lies between 6.154 and 11.96 and is greater than unity, indicating that lead(II) ions are favorably adsorbed by HQ-bentonite at all studied temperatures.

### 3.8. Thermodynamic parameters

The plot of $\ln K_L$ as a function of $1/T$ (Fig. 11) yields a straight line from which $\Delta H°$ and $\Delta S°$ were calculated from the slope and intercept, respectively. The thermodynamic results are tabulated in Table 3. The overall free energy changes during the adsorption process at all studied temperatures were negative, corresponding to a spontaneous process of lead(II) ions adsorption onto HQ-bentonite.

**Table 2**
Adsorption results of lead(II) ions from the literature by various clay-based adsorbents

| Adsorbent | Adsorption capacity (mg g$^{-1}$) |
|---|---|
| Illite [16] | 4.29 |
| Montmorillonite [17] | 31.05 |
| Poly(hydroxyl) zirconium-modified montmorillonite [17] | 31.44 |
| TBA-montmorillonite [17] | 30.67 |
| Natural bentonite [19] | 20.00 |
| Clinoptilolite [23] | 62.00 |
| Kaolinite [59] | 19.27 |
| Siderite [60] | 14.06 |
| Ballclay [61] | 3.52 |
| Coffee residue binding with clay [62] | 19.50 |
| Natural Jordanian clay [63] | 66.24 |
| Wollastonite [64] | 1.68 |
| 8-Hydroxy quinoline-immobilized bentonite (in this study) | 142.94 |
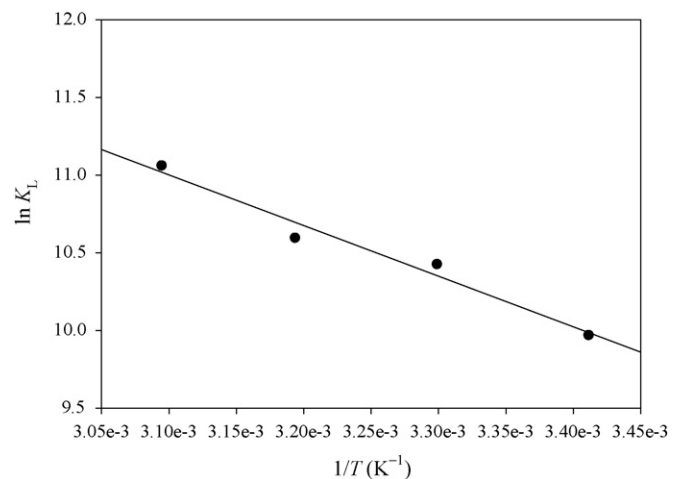


**Fig. 11.** Plot of $\ln K_L$ versus $1/T$ for the estimating of thermodynamic parameters for the adsorption of lead(II) ions onto HQ-bentonite.

**Table 3**
Thermodynamic parameters calculated from Langmuir isotherm constant ($K_L$) for the adsorption of lead(II) ions onto HQ-bentonite at various temperatures

| $t$ (°C) | $\Delta G°$ (kJ mol$^{-1}$) | $\Delta H°$ (kJ mol$^{-1}$) | $\Delta S°$ (J K$^{-1}$ mol$^{-1}$) |
|---|---|---|---|
| 20 | −24.30 | 27.12 | 175.54 |
| 30 | −26.28 | | |
| 40 | −27.59 | | |
| 50 | −29.72 | | |

The positive value of the enthalpy change (+27.12 kJ mol$^{-1}$) indicates that the adsorption is endothermic [65]. The positive entropy change ($\Delta S°$) value (+175.54 J mol$^{-1}$ K$^{-1}$) corresponds to an increase in randomness at the solid–liquid interface and maybe significant changes occur in the internal structure of the adsorbent through the adsorption of lead(II) ions on HQ-bentonite [6].

### 3.9. Adsorption kinetics

The Lagergren first-order, pseudo-second-order, Elovich and intraparticle diffusion kinetic models have been applied for the experimental data to analyze the adsorption kinetics of lead(II) ions. The plots of linear form of the Lagergren first-order (figure not shown), pseudo-second-order (Fig. 12), Elovich (figure not shown)
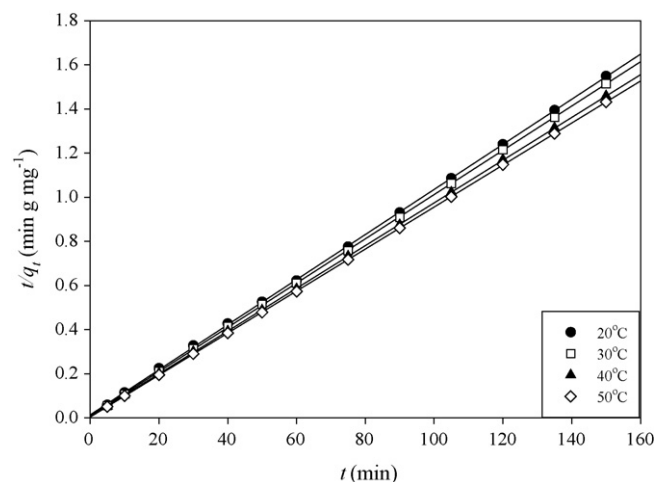


**Fig. 12.** Pseudo-second-order kinetic plots for the adsorption of lead(II) ions onto HQ-bentonite at various temperatures.
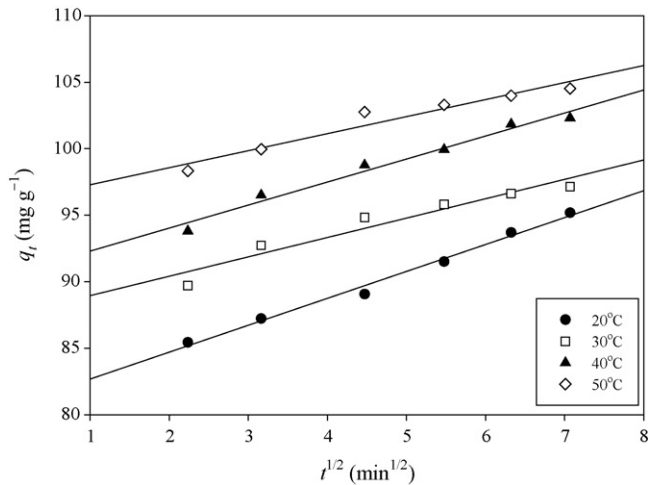
**Fig. 13.** Intraparticle diffusion plots for the adsorption of lead(II) ions onto HQ-bentonite at various temperatures.

and intraparticle diffusion (Fig. 13) for the adsorption of lead(II) ions were obtained at the temperatures of 20, 30, 40 and 50 °C. The kinetic parameters for the adsorption of lead(II) ions onto HQ-bentonite are summarized in Table 4. The plots of $\ln(q_1 - q_t)$ versus $t$ for the Lagergren first-order and the plots of $q_t$ versus $\ln(t)$ for the Elovich kinetic models are not shown as the figure due to the fact that the correlation coefficients for the Lagergren first-order and Elovich models are lower than that of the pseudo-second-order. Therefore, these imply that the adsorption of lead(II) ions onto HQ-bentonite does not follow the Lagergren first-order and Elovich kinetic models.

The correlation coefficients obtained are 0.999 for the pseudo-second-order model. These results imply that the adsorption follows to the pseudo-second-order kinetic model at all time intervals. The calculated $q_2$ values agree with experimental $q$ values, and also, the correlation coefficients for the pseudo-second-order kinetic plots were very high.

The correlation coefficients for the intraparticle diffusion model are lower than that of the pseudo-second-order kinetic model, whereas this model indicates that the adsorption of lead(II) ions HQ-bentonite may follow by the intraparticle diffusion model up to 60 min.

The pseudo-second-order rate constants indicate a steady increase from $7.37 \times 10^{-3}$ to $2.36 \times 10^{-2}$ g mg$^{-1}$ min$^{-1}$ with an
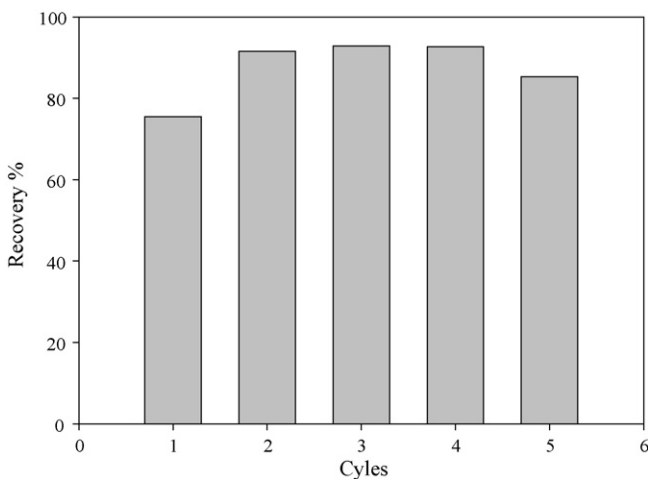


**Fig. 14.** The performance of HQ-bentonite by multiple cycles of regeneration.

**Table 4**
Kinetic parameters and the normalized standard deviations for the adsorption of lead(II) ions onto HQ-bentonite at various temperatures

| t (°C) | C_0 (mg dm$^{-3}$) | Lagergren first-order | | | | Pseudo-second-order | | | | Elovich | | | | Intraparticle diffusion | | | |
|---|---|---|---|---|---|---|---|---|---|---|---|---|---|---|---|---|---|
| | | $k_1$ (min$^{-1}$) | $q_1$ (mg g$^{-1}$) | $\Delta q$ (%) | $r_1^2$ | $k_2$ (g mg$^{-1}$ min$^{-1}$) | $q_2$ (mg g$^{-1}$) | $\Delta q$ (%) | $r_2^2$ | $\alpha$ (mg g$^{-1}$ min$^{-1}$) | $\beta$ (g mg$^{-1}$) | $\Delta q$ (%) | $r_E^2$ | $k_p$ (mg g$^{-1}$ min$^{-1/2}$) | $C$ (mg g$^{-1}$) | $\Delta q$ (%) | $r_p^2$ |
| 20 | 100 | $7.88 \times 10^{-2}$ | 21.05 | – | 0.881 | $1.29 \times 10^{-2}$ | 86.96 | 1.265 | 0.999 | $3.31 \times 10^{11}$ | 0.348 | 3.856 | 0.890 | 1.727 | 73.72 | 3.439 | 0.846 |
| | 112.5 | $6.09 \times 10^{-2}$ | 22.96 | – | 0.958 | $7.37 \times 10^{-3}$ | 97.91 | 1.815 | 0.999 | $3.57 \times 10^{9}$ | 0.261 | 3.365 | 0.940 | 1.024 | 80.65 | 4.139 | 0.991 |
| | 125 | $6.25 \times 10^{-2}$ | 29.76 | – | 0.942 | $6.57 \times 10^{-3}$ | 100.63 | 1.409 | 0.999 | $1.24 \times 10^{9}$ | 0.243 | 4.927 | 0.962 | 1.995 | 82.79 | 2.836 | 0.973 |
| | 150 | $2.73 \times 10^{-2}$ | 13.50 | – | 0.825 | $5.77 \times 10^{-3}$ | 108.80 | 1.622 | 0.999 | $3.25 \times 10^{8}$ | 0.211 | 2.089 | 0.944 | 2.602 | 87.25 | 2.475 | 0.902 |
| 30 | 112.5 | $5.29 \times 10^{-2}$ | 14.82 | – | 0.943 | $1.07 \times 10^{-2}$ | 99.73 | 1.635 | 0.999 | $1.27 \times 10^{14}$ | 0.365 | 1.713 | 0.958 | 1.456 | 87.49 | 2.619 | 0.932 |
| 40 | 112.5 | $5.41 \times 10^{-2}$ | 11.02 | – | 0.885 | $1.48 \times 10^{-2}$ | 103.30 | 1.272 | 0.999 | $2.23 \times 10^{15}$ | 0.379 | 1.338 | 0.907 | 1.730 | 90.57 | 2.048 | 0.978 |
| 50 | 112.5 | $5.40 \times 10^{-2}$ | 5.402 | – | 0.853 | $2.36 \times 10^{-2}$ | 105.07 | 1.306 | 0.999 | $9.45 \times 10^{22}$ | 0.542 | 3.351 | 0.876 | 1.280 | 96.00 | 1.519 | 0.943 |
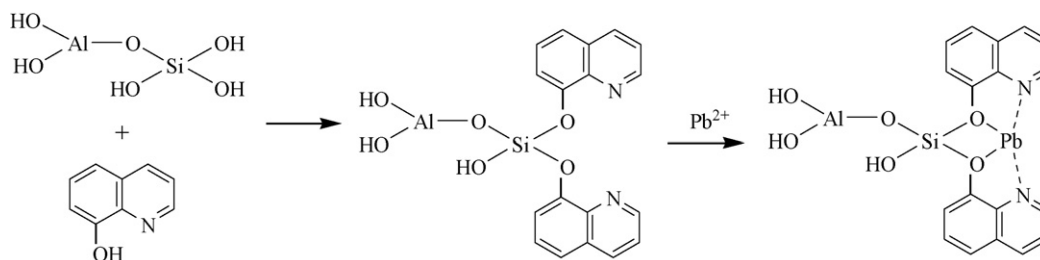
**Fig. 15.** The possible mechanism for the adsorption of lead(II) ions onto 8-hydroxy quinoline-immobilized bentonite.

increase in the solution temperatures from 20 to 50 °C (Table 4) and at the initial lead(II) ions concentration of 112.5 mg dm$^{-3}$, indicating that the adsorption of lead(II) ions onto HQ-bentonite is the rate-controlled.

The validity of kinetic models in this study can be controlled by using Eq. (12) and the calculated results are listed in Table 4. As it can be seen from Table 4, the values of $\Delta q$ (%) for the best-fit model are less than 1.816%. It is concluded that the adsorption of lead(II) ions onto HQ-bentonite can be best described by the pseudo-second-order kinetic model.

### 3.10. Regeneration

The regenerated adsorbent was reused for up to five adsorption–desorption cycles and the results are illustrated in Fig. 14. From this figure, it was clear that the efficiency of lead(II) ions (adsorption–desorption) process was nearly the same as the cycles of two to four and dropped a little in the fifth cycle. This might be due to the ignorable amount of adsorbent lost during the adsorption–desorption process. The decline in efficiency was not more than 8% which showed that the adsorbent had a good potential to adsorb lead(II) ions although it has been reused for five times. The regeneration of adsorbent with 0.1 M HCl showed that the adsorption–desorption process using HQ-bentonite was a reversible process.

### 3.11. Suggested lead(II) ions adsorption mechanism with 8-hydroxy quinoline-immobilized bentonite

The silanol groups in bentonite are the responsible for the immobilization of natural bentonite. The immobilization agent, 8-hydroxy quinoline, was used in this work and HQ-bentonite was then examined as an adsorbent for the adsorption of lead(II) ions from aqueous solution. The results show that HQ-bentonite can easily adsorb lead(II) ions a possible mechanism by using silanol –OH groups as can be seen from Fig. 15.

### 4. Conclusions

In this study, the adsorption of lead(II) ions onto HQ-bentonite in aqueous solutions was investigated. It may be summarized that HQ-bentonite acts a respective adsorbent for the removal of lead(II) ions in aqueous solutions because of its high adsorption capacity. The maximum adsorption capacity was found to be 142.94 mg g$^{-1}$ at pH 5.5 and 50 °C.

The functional groups of natural bentonite, HQ-bentonite and lead(II)-loaded HQ-bentonite were identified by using FTIR spectrophotometer. The isoelectric point (pH$_{pzc}$) of HQ-bentonite in lead(II) ions solution was determined as 3.28.

The straight lines obtained for the Langmuir, Freundlich and Dubinin–Radushkevich (D–R) isotherm models obey to fit to the experimental equilibrium data, whereas the Langmuir isotherm model gives better fittings than other isotherm models. The thermodynamic parameters obtained from Langmuir constant ($K_L$) indicate feasible, spontaneous and endothermic adsorption.

The pseudo-second-order kinetic model agrees very well with the dynamic behavior for the adsorption of lead(II) ions onto HQ-bentonite at various temperatures. The experimental data have also been applied to estimate the rate constants of adsorption. However, the evidence is provided that the adsorption of lead(II) ions onto HQ-bentonite is a complex process, therefore it cannot be sufficiently described by a single kinetic model throughout the whole process. For example, the intraparticle diffusion (up to 60 min) played a significant role, however it was not the main rate-determining step during the adsorption process. The regeneration and subsequent use of HQ-bentonite would also enhance the economics of adsorption of lead(II) ions from pollutants.

### References

[1] C.L. Ake, K. Mayura, H. Huebner, G.R. Bratton, T.D. Phillips, Development of porous clay-based composites for the sorption of lead from water, J. Toxicol. Environ. Health Part A 63 (6) (2001) 459–475.
[2] S. Tunali, T. Akar, A.S. Özcan, I. Kiran, A. Özcan, Equilibrium and kinetics of biosorption of lead(II) from aqueous solutions by *Cephalosporium aphidicola*, Sep. Purif. Technol. 47 (3) (2006) 105–112.
[3] A. Kapoor, T. Viraraghavan, D.R. Cullimore, Removal of heavy metals using the fungus *Aspergillus niger*, Bioresour. Technol. 70 (1) (1999) 95–104.
[4] W. Lo, H. Chua, K.H. Lam, S.P. Bi, A comparative investigation on the biosorption of lead by filamentous fungal biomass, Chemosphere 39 (15) (1999) 2723–2736.
[5] B. Volesky, Detoxification of metal-bearing effluents: biosorption for the next century, Hydrometallurgy 59 (2–3) (2001) 203–216.
[6] A.S. Özcan, A. Özcan, Adsorption of acid dyes from aqueous solutions onto acid-activated bentonite, J. Colloid Interface Sci. 276 (1) (2004) 39–46.
[7] A.S. Özcan, B. Erdem, A. Özcan, Adsorption of Acid Blue 193 from aqueous solutions onto Na-bentonite and DTMA-bentonite, J. Colloid Interface Sci. 280 (1) (2004) 44–54.
[8] H. Ucun, Y.K. Bayhan, Y. Kaya, A. Cakici, O.F. Algur, Biosorption of lead(II) from aqueous solution by cone biomass of *Pinus sylvestris*, Desalination 154 (3) (2003) 233–238.
[9] C.P. Huang, C.P. Huang, A.L. Morehart, The removal of Cu(II) from dilute aqueous solutions by *Saccharomyces cerevisiae*, Water Res. 24 (4) (1990) 433–439.
[10] Z.R. Holan, B. Volesky, Biosorption of lead and nickel by biomass of marine algae, Biotechnol. Bioeng. 43 (11) (1994) 1001–1009.
[11] W. Jianlong, Z. Xinmin, D. Decai, Z. Ding, Bioadsorption of lead(II) from aqueous solution by fungal biomass of *Aspergillus niger*, J. Biotechnol. 87 (3) (2001) 273–277.
[12] E. Fourest, J.C. Roux, Heavy metal biosorption by fungal mycelial by-products: mechanism and influence of pH, Appl. Microbiol. Biotechnol. 37 (3) (1992) 399–403.
[13] S. Tunali, A. Çabuk, T. Akar, Removal of lead and lead(II) ions from aqueous solutions by bacterial strain isolated from soil, Chem. Eng. J. 115 (3) (2006) 203–211.
[14] S.K. Srivastava, R. Tyagi, N. Pant, N. Pal, Studies on the removal of some toxic metal ions. Part II. Removal of lead and cadmium by montmorillonite and kaolinite, Environ. Technol. (Lett.) 10 (3) (1989) 275–282.
[15] F.F.O. Orumwense, Removal of lead from water by adsorption on a kaolinitic clay, J. Chem. Technol. Biotechnol. 65 (4) (1996) 363–369.
[16] V. Chantawong, N.W. Harvey, V.N. Bashkin, Adsorption of lead nitrate on Thai kaolin and ballclay, Asian J. Energy Environ. 2 (1) (2001) 33–48.
[17] S.S. Gupta, K.G. Bhattacharyya, Interaction of metal ions with clays. I. A case study with Pb(II), Appl. Clay Sci. 30 (3–4) (2005) 199–208.
[18] J.C. Echeverría, I. Zarranz, J. Estella, J.J. Garrido, Simultaneous effect of pH, temperature, ionic strength, and initial concentration on the retention of lead on illite, Appl. Clay Sci. 30 (1) (2005) 103–115.

[19] R. Naseem, S.S. Tahir, Removal of Pb(II) from aqueous/acidic solutions by using bentonite as an adsorbent, Water Res. 35 (16) (2001) 3982–3986.
[20] R. Donat, A. Akdogan, E. Erdem, H. Cetisli, Thermodynamics of $Pb^{2+}$ and $Ni^{2+}$ adsorption onto natural bentonite from aqueous solutions, J. Colloid Interface Sci. 286 (1) (2005) 43–52.
[21] F. Barbier, G. Duc, M. Petit-Ramel, Adsorption of lead and cadmium ions from aqueous solution to the montmorillonite/water interface, Colloids Surf. A: Physicochem. Eng. Aspects 166 (1–3) (2000) 153–159.
[22] M.J. Zamzow, B.R. Eichbaum, K.R. Sandgren, D.E. Shanks, Removal of heavy metals and other cations from wastewater using zeolites, Sep. Sci. Technol. 25 (13–15) (1990) 1555–1569.
[23] S.K. Ouki, C. Cheeseman, R. Perry, Effects of conditioning and treatment of chabazite and clinoptilolite prior to lead and cadmium removal, Environ. Sci. Technol. 27 (6) (1993) 1108–1116.
[24] M.F. Brigatti, C. Lugli, L. Poppi, Kinetics of heavy-metal removal and recovery in sepiolite, Appl. Clay Sci. 16 (1–2) (2000) 45–57.
[25] N. Bektaş, B.A. Ağım, S. Kara, Kinetic and equilibrium studies in removing lead ions from aqueous solutions by natural sepiolite, J. Hazard. Mater. 112 (1–2) (2004) 115–122.
[26] R.S. Juang, S.H. Lin, K.H. Tsao, Mechanism of sorption of phenols from aqueous solutions onto surfactant-modified montmorillonite, J. Colloid Interface Sci. 254 (2) (2002) 234–241.
[27] F.A. Banat, B. Al-Bashir, S. Al-Asheh, O. Hayajneh, Adsorption of phenol by bentonite, Environ. Pollut. 107 (3) (2000) 391–398.
[28] Y.-H. Shen, Preparation of organobentonite using non-ionic surfactants, Chemosphere 44 (5) (2001) 989–995.
[29] I. Langmuir, The adsorption of gases on plane surfaces of glass, mica and platinum, J. Am. Chem. Soc. 40 (9) (1918) 1361–1403.
[30] H.M.F. Freundlich, Über die adsorption in lösungen, Z. Phys. Chem. 57 (1906) 385–470.
[31] M.M. Dubinin, L.V. Radushkevich, Proc. Acad. Sci. U.S.S.R. Phys. Chem. Sect. 55 (1947) 331–333.
[32] K.R. Hall, L.C. Eagleton, A. Acrivos, T. Vermeulen, Pore- and solid-diffusion kinetics in fixed-bed adsorption under constant-pattern conditions, Ind. Eng. Chem. Fundam. 5 (2) (1966) 212–223.
[33] S. Lagergren, Zur theorie der sogenannten adsorption gelöster stoffe, Kungliga Svenska Vetenskapsakademiens, Handlingar 24 (4) (1898) 1–39.
[34] Y.S. Ho, G. McKay, Kinetic models for the sorption of dye from aqueous solution by wood, J. Environ. Sci. Health Part B: Process Safety Environ. Protect. 76 (B2) (1998) 183–191.
[35] M.J.D. Low, Kinetics of chemisorption of gases on solids, Chem. Rev. 60 (1960) 267–312.
[36] S.H. Chien, W.R. Clayton, Application of Elovich equation to the kinetics of phosphate release and sorption in soils, Soil Sci. Soc. Am. J. 44 (1980) 265–268.
[37] D.L. Sparks, Kinetics and mechanisms of chemical reactions at the soil mineral/water interface, in: D.L. Sparks (Ed.), Soil Physical Chemistry, CRC Press, Boca Raton, Florida, 1999, pp. 135–192.
[38] W.J. Weber Jr., J.C. Morriss, Kinetics of adsorption on carbon from solution, J. Sanitary Eng. Div. Am. Soc. Civ. Eng. 89 (1963) 31–60.
[39] A. Özcan, A.S. Özcan, Adsorption of Acid Red 57 from aqueous solutions onto surfactant-modified sepiolite, J. Hazard. Mater. 125 (1–3) (2005) 252–259.
[40] A.S. Özcan, Ş. Tetik, A. Özcan, Adsorption of acid dyes from aqueous solutions onto sepiolite, Separ. Sci. Technol. 39 (2) (2004) 301–320.
[41] K.G. Bhattacharyya, A. Sharma, *Azadirachta indica* leaf powder as an effective biosorbent for dyes: a case study with aqueous Congo Red solutions, J. Environ. Manage. 71 (3) (2004) 217–229.
[42] J.P. Chen, S. Wu, K.H. Chong, Surface modification of a granular activated carbon by citric acid for enhancement of copper adsorption, Carbon 41 (10) (2003) 1979–1986.
[43] F.-C. Wu, R.-L. Tseng, R.-S. Juang, Kinetic modeling of liquid-phase adsorption of reactive dyes and metal ions on chitosan, Water Res. 35 (3) (2001) 613–618.
[44] R.K. Taylor, Cation exchange in clays and mudrocks by methylene blue, J. Chem. Technol. Biotechnol. 35A (1985) 195–207.
[45] G. Akçay, M. Akçay, K. Yurdakoç, Removal of 2,4-dichlorophenoxyacetic acid from aqueous solutions by partially characterized organophilic sepiolite: thermodynamic and kinetic calculations, J. Colloid Interface Sci. 281 (1) (2005) 27–32.
[46] R.M. Silverstein, F.X. Webster, Spectrometric Identification of Organic Compounds, 6th ed., J. Wiley, New York, 1998.
[47] A. Delgado, F. González-Caballero, J.M. Bruque, On the zeta potential and surface charge density of montmorillonite in aqueous electrolyte solutions, J. Colloid Interface Sci. 113 (1) (1986) 203–211.
[48] Y. Horikawa, R.S. Murray, J.P. Quirk, The effect of electrolyte concentration on the zeta potentials of homoionic montmorillonite and illite, Colloids Surf. 32 (1988) 181–195.
[49] D.J.A. Williams, K.P. Williams, Electrophoresis and zeta potential of kaolinite, J. Colloid Interface Sci. 65 (1) (1978) 79–87.
[50] A. Chakir, J. Bessiere, K.E.L. Kacemi, B. Marouf, A comparative study of the removal of trivalent chromium from aqueous solutions by bentonite and expanded perlite, J. Hazard. Mater. 95 (1–2) (2002) 29–46.
[51] J.S. Laskowski, Electrokinetic measurements in aqueous solutions of weak electrolyte type surfactants, J. Colloid Interface Sci. 159 (2) (1993) 349–353.
[52] E. Günister, N. Güngör, Ö.I. Ece, The investigations of influence of BDTDACl and DTABr surfactants on rheologic, electrokinetic and XRD properties of Na-activated bentonite dispersions, Mater. Lett. 60 (2006) 666–673.
[53] R.J. Hunter, Zeta Potential in Colloid Science: Principles and Applications, Academic Press, UK, 1988.
[54] C.F. Baes Jr., R.E. Mesmer, The Hydrolysis of Cations, John Wiley and Sons, New York, 1976.
[55] K. Zhang, W.H. Cheung, M. Valix, Roles of physical and chemical properties of activated carbon in the adsorption of lead ions, Chemosphere 60 (8) (2005) 1129–1140.
[56] Y. Qiu, H. Cheng, C. Xu, G.D. Sheng, Surface characteristics of crop-residue-derived black carbon and lead(II) adsorption, Water Res. 42 (2008) 567–574.
[57] M.S. Alhakawati, C.J. Banks, Removal of copper from aqueous solution by *Ascophyllum nodosum* immobilised in hydrophilic polyurethane foam, J. Environ. Manage. 72 (4) (2004) 195–204.
[58] Z. Aksu, E. Kabasakal, Batch adsorption of 2,4-dichlorophenoxy-acetic acid (2,4-D) from aqueous solution by granular activated carbon, Sep. Purif. Technol. 35 (3) (2004) 223–240.
[59] K.O. Adebowale, I.E. Unuabonah, B.I. Olu-Owolabi, The effect of some operating variables on the adsorption of lead and cadmium ions on kaolinite clay, J. Hazard. Mater. 134 (1–3) (2006) 130–139.
[60] M. Erdem, A. Özverdi, Lead adsorption from aqueous solution onto siderite, Sep. Purif. Technol. 42 (3) (2005) 259–264.
[61] V. Chantawong, N.W. Harvey, V.N. Bashkin, Comparison of heavy metal adsorptions by Thai kaolin and ballclay, Water Air Soil Poll. 148 (1–4) (2003) 111–125.
[62] V. Boonamnuayvitaya, C. Chaiya, W. Tanthapanichakoon, S. Jarudilokkul, Removal of heavy metals by adsorbent prepared from pyrolyzed coffee residues and clay, Sep. Purif. Technol. 35 (1) (2004) 11–22.
[63] Y.S. Al-Degs, M.I. El-Barghouthi, A.A. Issa, M.A. Khraisheh, G.M. Walker, Sorption of Zn(II), Pb(II), and Co(II) using natural sorbents: equilibrium and kinetic studies, Water Res. 40 (14) (2006) 2645–2658.
[64] K.P. Yadava, B.S. Tyagi, V.N. Singh, Effect of temperature on the removal of Pb(II) adsorption on china clay and wollastonite, J. Chem. Technol. Biotechnol. 51 (1991) 47–60.
[65] Y. Yu, Y.-Y. Zhuang, Z.-H. Wang, Adsorption of water-soluble dye onto functionalized resin, J. Colloid Interface Sci. 242 (2) (2001) 288–293.